PERGAMON

International Journal of Heat and Mass Transfer 44 (2001) 3701–3708

International Journal of HEAT and MASS TRANSFER

www.elsevier.com/locate/ijhmt

Near wake of a circular cylinder submitted to blowing – I Boundary layers evolution

L. Mathelin, F. Bataille, A. Lallemand *

Institut National des Sciences Appliquées de Lyon, Centre de Thermique de Lyon, UMR 5008, Bât. S. Carnot, 20 Avenue Albert Einstein, 69621 Villeurbanne Cedex, France

Received 20 July 2000; received in revised form 23 November 2000

Abstract

The dynamical and thermal behavior of the flow around a circular cylinder submitted to blowing is experimentally investigated. The blowing is applied through the whole surface of a porous cylinder submitted to a heated turbulent main fluid in cross-flow. Velocity, pressure and temperature profiles are determined for different injection rates and main flow temperatures for Reynolds numbers ranging from 3900 to 14 000. The velocity and temperature profiles are similarly modified with the blowing, while the injection thickens the boundary layers and modifies their shape. These evolutions lower the transfer coefficients, both dynamical (shear stress) and thermal (heat transfer), and are dependent on the location around the cylinder. The blowing impact on the wall temperature is also quantified, exibiting an excellent effectiveness of the cooling with blowing.

1. Introduction

The bluff body surface temperature reduction is of primary interest for many applications and allows for higher main flow temperatures while keeping the wall thermal stress to a reasonable level. When used in aircraft engines, the overall output can be significantly improved with a higher combustion temperature and crucial mechanical parts lifespan can be lengthened if better protected (rocket nozzle). Many ways of protecting wall have been studied in the past. Internal heat convection is used for low thermally stressed bodies as can be found in certain turbine stages. When higher thermal protection is required, other techniques are employed such as film cooling or discrete injection through small holes drilled in an impermeable material [1–4]. The injection angle can be inclined (film cooling) or normal (discrete injection). Most of the high thermally stressed parts are protected with these techniques. Blowing consists in injecting a secondary fluid through a porous surface, which represents the limit case of film cooling. In 1953, Eckert and Livingood [5] proposed an approximate theoretical method, based on a similarity to wedge flows, for predicting the thermal performance of the complete blowing through a circular cylinder while Johnson and Hartnett [6] experimentally studied the convective heat flux density as a function of the angle and the blowing for a few Reynolds numbers. Since then, no major work has been done and more data are required. In particular, a detailed study of the dynamical and thermal fields near the cylinder surface, included beyond the separation point and the recirculation zone, would be of fundamental interest. It has already been proved that complete blowing is more efficient, in terms of coolant mass flow rate required for a same protection, than discrete blowing [7]. Despite its undoubtful superiority, mechanical strength problems and the research effort still required for its achievement have delayed its use in practical applications such as aircraft engines for example. Hence, little experimental, as well as theoretical or numerical data are available up to now concerning the complete blowing around a bluff body.

Besides the thermal point of interest, blowing from a surface has also been studied for circulation, lift and viscous drag control [8–12]. Associated with localized suction, the blowing can significantly reduce the drag,

* Corresponding author. Tel.: +33-4-7243-8232; fax: +33-4-7243-6010.

E-mail address: a.lal@cethil.insa-lyon.fr (A. Lallemand).

0017-9310/01/$ - see front matter
PII: S0017-9310(01)00020-5

Nomenclature

dx	elementary streamwise length
dy	elementary transverse length
D	cylinder outer diameter
F	blowing rate, $(\rho_{inj}U_{inj})/(\rho_\infty U_\infty)$
h	transverse distance to the wall
Re	Reynolds number, $\rho_\infty U_\infty D/\mu_\infty$
T	temperature
U	fluid velocity magnitude
x	streamwise coordinate
y	transverse coordinate
z	spanwise coordinate

Greek symbols

δ	dynamical boundary layer thickness
Δ	thermal boundary layer thickness
η	thermal effectiveness, $(T_\infty - T)/(T_\infty - T_{inj})$
θ	angle referred from the front stagnation point
μ	fluid dynamic viscosity
ρ	fluid density

Subscripts

∞	upstream properties
inj	injected fluid

decreasing the shear stress in the upstream part of the bluff body, while the suction at the downstream side delays the boundary layer separation and narrows the wake.

The aim of the present investigation is to describe how the complete blowing (i.e., through the whole surface of a cylinder) can modify some basic features of the flow around a circular cylinder. This blowing impact can be dynamical (boundary layers) as well as thermal (wall temperature, thermal stress). After a presentation of the experimental facilities in Section 2, the drastical influence of the blowing on the profiles shape and the modification of the separation conditions is addressed in Section 3. The surface temperature evolution with blowing is finally presented in Section 4.

2. Experimental facilities

Experiments are conducted in a heated subsonic wind tunnel with a test section consisting in a 0.2 m × 0.5 m rectangular cross-section. Throughout the velocity range $[0;30]$ m s^{-1} attainable, the residual velocity turbulence intensity has been measured to be always below 1% in the mainstream but results cannot be considered as completely free from turbulence effects. Thermal control is ensured by heating needles driven by a PID regulator. The mainflow temperature can vary from ambient to 250°C, thanks to a 120 kW electrical heating power. A schematic description of the set-up can be seen in Fig. 1 (see Rodet et al. [13] for more details). A 16.2 mm outer diameter, 2.1 mm thick, 320 mm long, hollow circular cylinder (pipe) was set horizontally in the centerline of the test section. Aspect and blockage ratii are 20% and 8%, respectively. The cylinder, made of sintered-stainless-steel, 30% porosity and 30 μm average pore diameter, can be fed at the ends by a secondary, vane-adjusted, flow (coolant). Blowing uniformity is ensured by the ratio between the pressure loss through the porous material and the front and rear stagnation points pressure difference. This ratio is always larger than 1000 for all experiments, thus allowing a reliable blowing

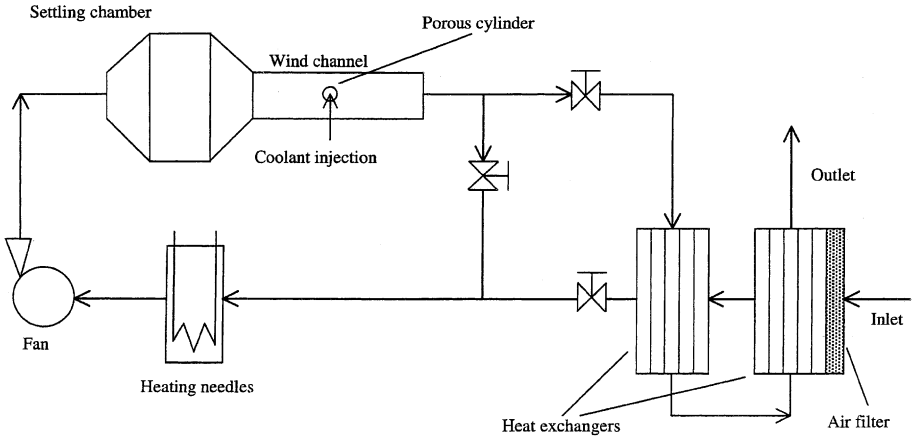

Fig. 1. Schematic of the experimental wind tunnel.

uniformity for the whole surface. Pressure variations along the stream within the pipe are negligible as well, as can be found using the Bernoulli's equation. A porous disk, inserted inside the secondary air pipe, prevents from spurious upstream high frequency pressure oscillations. Three-dimensional and end effects were studied through tests conducted using end plates. They are oblong shaped, consisting in a rectangle featuring 5 D in length upstream to the cylinder axis, 15 D downstream and 10 D in height, D being the outer cylinder diameter. They can be inclined with respect to the upstream flow in order to study the shedding angle impact on results. The velocity was measured with a single hot-wire Dantec 55P11-2 probe. This probe was used because of the very small size of the boundary layers investigated (see below), which makes measurements impossible with an X-wire probe. Furthermore, an X-wire probe is much more intrusive and more likely to distort the flow in the immediate vicinity of the wall. Hence, only the velocity magnitude measurement is possible. The wire is made of 10% rhodium–platinum, 10 μm in diameter, about 1.5 mm in length and has a good frequency response up to, at least, 3 kHz. For the temperature profiles, a single 5 μm in diameter Wollaston (platinum–rhodium core and silver coating) cold-wire probe was used.

A fourth-order polynomial form was assumed for the velocity and the wire output voltage (derived from King's law [14]) and a quadratic form was applied for the cold-wire probe. The quadratic form for the calibration evolution with the temperature is derived from the quasi-linear behavior of the cold-wire resistance. Small non-linearities are accounted in a second-order term. The coefficients are determined using a least-squares method. For the velocity calibration, a polynom is determined for several mainstream temperatures (five typically). From these five $\mathbb{R}$ polynoms, a regressed $\mathbb{R}^2$ polynom, quadratic in temperature, is determined and finally used for velocity measurements whatever the temperature. These methods have already been used for several measurements above a flat porous plate submitted to blowing, using hot and cold wires, leading to concluant results [15].

The hot-wire probe is driven by a 90C10 CTA Dantec module and data are acquired on a PC through an AT-MIO-16E10 National Instruments A/D card. The probe body is vertical, in cross-flow, ending with 5 mm long probe terminals and the wire axis is parallel to the cylinder axis. The experimental arrangement can be seen in Fig. 2. Hot-wires probes are calibrated in velocity with a Pitot tube combined with a high sensitivity Furness FCO332 differential pressure transmitter. Its accuracy is better than 1% of the measured value throughout its [0–100] Pa range with a 0.1 Pa resolution. The wall cylinder temperature is measured with K-type thermocouples welded onto the surface around the circumference. Using an IR camera, they have previously been proved not to disrupt the temperature field of the porous surface [16]. The Reynolds number is based on the cylinder diameter D and upstream fluid properties:

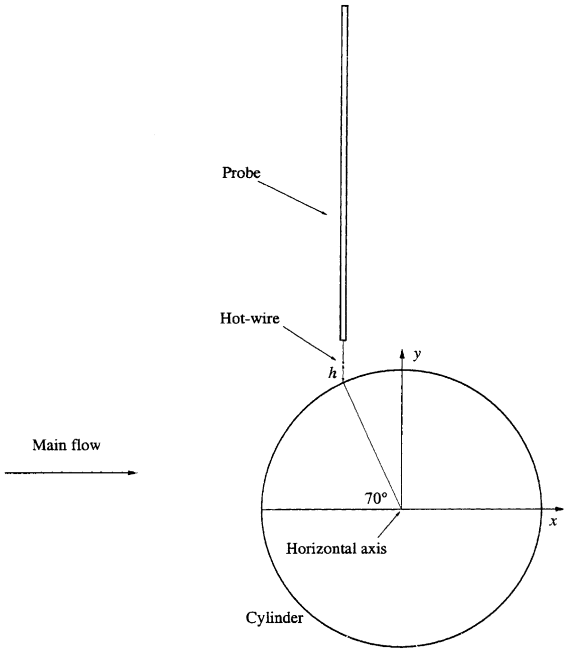

Fig. 2. Sketch of the probe arrangement.

$$Re = \frac{\rho_\infty D U_\infty}{\mu_\infty}$$

and has an uncertainty varying between 0.7% and 5.5%. The blowing ratio, or injection rate, F, represents the amount of coolant injected in comparison to the main flow rate. It is defined as

$$F = \frac{\rho_{\text{inj}} U_{\text{inj}}}{\rho_\infty U_\infty},$$

where ρ is the density, U the velocity, subscript inj refers to the injected fluid and ∞ to the main fluid. Its uncertainty is estimated to be typically of 7% and always lower than 10% for all experimental conditions.

3. Impact on the boundary layers

3.1. Dynamical profiles

We are interested in determining the influence of the blowing on the temperature and velocity profiles. Two different Reynolds numbers are investigated (3900 and 7000). The study of the blowing influence on the velocity profiles is carried out in an isothermal configuration, i.e., the temperature of the injected and main flow remains at 20°C. For the investigation of the temperature profiles,

the main flow temperature is varied from ambient temperature to 250°C. Nevertheless, for weak injection rates, the coolant is heated while flowing through the porous matrix, and the blown air temperature can be significantly higher than 20°C. The injection rate is varied from 0% to 10%. The velocity and temperature profiles are determined at three different positions around the cylinder. The first one is located at an angle θ of 70°, originated from the front stagnation point, which corresponds to a location upstream to the separation point. The second one is at 90°, and the third one is at 110°, far beyond the separation point.

Fig. 3 shows the velocity profiles for an angle of 70° and a Reynolds number of 3900 for three different injection rates. Spatial variables are x, y and z for the streamwise, transverse and spanwise coordinates, respectively, the origin being the midspan point on the cylinder axis. For the sake of experimental convenience, the profiles are plotted along the vertical direction for all angles. It thus represents a profile along the normal direction when $\theta = 90°$ only. The height variable, h, is referred from the surface and is non-dimensionalized with the cylinder diameter D. Even in the case of strong injection, the velocity profile clearly indicates that the boundary layer remains attached due to the finite velocity magnitude normal gradient at the surface. When blowing occurs, it can be observed that its thickness is increased. For a constant h/D position, the velocity magnitude is reduced all the more that the injection rate increases and, simultaneously, the profile tends to become linear in the boundary layer. Similar trends were observed above a porous flat plate [17]. Consequently, boundary layers with negative pressure gradients upstream to the separation point seem to behave similarly to flat plate boundary layers when injection occurs. Similar conclusions can be drawn from Fig. 4 where the same velocity profiles are plotted for a Reynolds number of 7000. Here again, the friction stress decreases, due to a lower normal velocity gradient at the surface, and the boundary layer thickness dramatically increases with blowing.

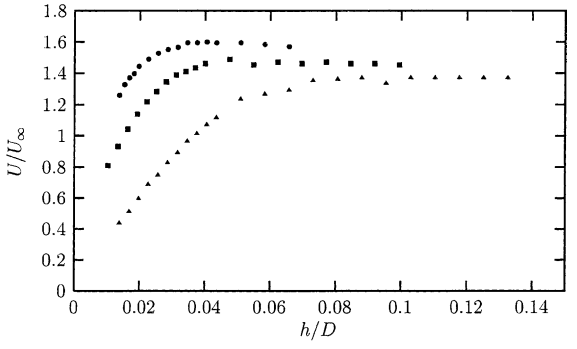

Fig. 3. Velocity magnitude profile along the vertical direction. $Re = 3900$, $\theta = 70°$. ●, $F = 0\%$; ■, $F = 2\%$; ▲, $F = 5\%$.

Because of interference risks due to the presence of the hot wire, measurements were intentionally limited to a finite distance from the wall. For a Reynolds number of 7000, the boundary layer thickness is about 600 μm at an angle of 70°. Considering at least 10 measurement points, equally spaced within the boundary layer, leads to a first point 60 μm above the wall, while the wire diameter is 10 μm. This could result in spurious values in addition to difficulties in handling the probe. Hence, the velocity profiles are truncated below a certain distance from the surface. Furthermore, for very low velocities, the differential pressure transmitter resolution does not allow for reliable velocity calibration and leads to spurious values in the velocity profiles. Hereagain, the velocity profiles are thus to be truncated to a minimum velocity. In particular, the dead fluid region cannot be explicitly plotted as the velocity signal delivered by the probe conditioner is below the reliable calibration range.

The velocity profiles for $\theta = 90°$ at $Re = 7000$ are shown in Fig. 5. In the vicinity of the wall, the profile shape is rather different from that at 70° due to the adverse pressure gradient. When blowing occurs, it tends to an S-shaped-like profile exhibiting the promotion of

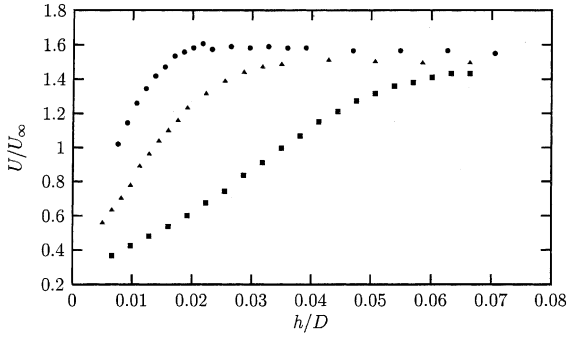

Fig. 4. Velocity magnitude profile along the vertical direction. $Re = 7000$, $\theta = 70°$. ●, $F = 0\%$; ■, $F = 2\%$; ▲, $F = 5\%$.

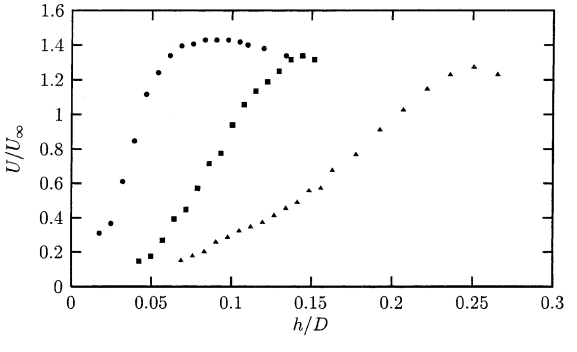

Fig. 5. Velocity magnitude profile along the vertical direction. $Re = 7000$, $\theta = 90°$. ●, $F = 0\%$; ■, $F = 2\%$; ▲, $F = 4\%$.

the separation. This tendency is reinforced at higher injection rates. In the literature, the value of the separation angle reported is around 88° for a smooth impermeable cylinder in this range of Reynolds number [18]. In the no-blowing case, we found a slightly higher value as the cylinder surface has a 50 μm high roughness, which delays the separation. With blowing, the separation of the boundary layer is considerably promoted as can be observed from the dead region size (where the velocity profile is flat and very low), which becomes larger. In particular, in Fig. 5, the dead region height is doubled for a 2% injection rate and almost multiplied by a factor of 3 for a 5% injection rate. Applying blowing thus tends to push away the main flow and, for high injection rates, the cylinder becomes completely isolated from the primary flow.

In Table 1, the boundary layer thickness δ, defined as the height where the flow velocity is 99% of the maximum velocity to account for the potential velocity distribution, is reported as a function of the injection rate for an angle of 70° and a Reynolds number of 3900 and 7000. These results illustrate the strong influence of the blowing on the boundary layer and the near wall flow behavior. For 2% of injection, the thickness is increased by 70%, whereas for 4% it rises up to 170%.

Figs. 6 and 7 show the velocity magnitude profile at a Reynolds number of 3900 and 7000, respectively, for $\theta = 110°$. Profiles are limited to the separated boundary layer itself, hereafter considered as a shear layer, without

Table 1
Dynamical boundary layer thickness evolution with blowing ($Re = 3900$ and 7000, $\theta = 70°$)

F (%)	δ/D	
	$Re = 3900$	$Re = 7000$
0	0.04	0.02
2	0.05	0.04
5	0.08	0.07

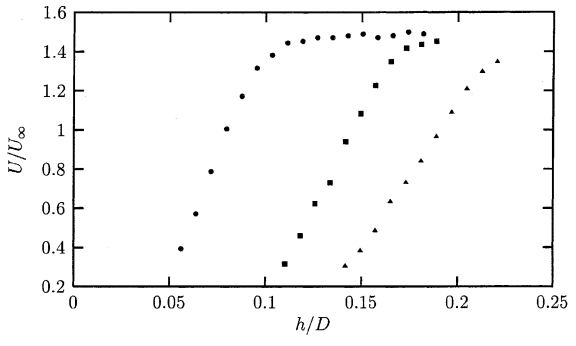

Fig. 6. Velocity magnitude profile along the vertical direction. $Re = 3900$, $\theta = 110°$. •, $F = 0\%$; ▪, $F = 2\%$; ▲, $F = 5\%$.

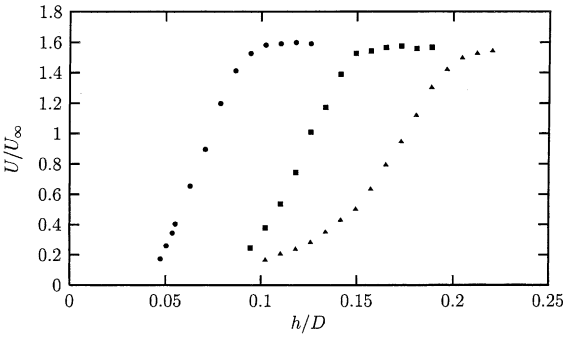

Fig. 7. Velocity magnitude profile along the vertical direction. $Re = 7000$, $\theta = 110°$. •, $F = 0\%$; ▪, $F = 2\%$; ▲, $F = 5\%$.

exploring further. The blowing impact remains the same on a shear layer as on an attached boundary layer, i.e., an increase in its thickness due to lower gradients and a larger dead fluid height. A similar dynamical evolution with blowing is obtained for the two values of Reynolds number (Figs. 6 and 7) and the two curves collapse if normalized with the boundary layer thickness (not shown here for sake of brevity). It demonstrates that the Reynolds number does not act in this range where the profiles are similar from a mathematical point of view.

Furthermore, the study of the main flow temperature influence on the velocity profiles has been conducted. The main flow temperature was varied from ambient to 200°C, while keeping F constant. No appreciable difference on the velocity profiles can be noted, confirming the fact that F is the correct control parameter to account for the blowing impact.

A current way of studying the near wake flow is to plot the pressure coefficient along the cylinder surface. This would have been interesting but it is rather impossible in our configuration. A pressure probe drilled in the wall would have blocked some porous area and would strongly affect the outer dynamics, leading to spurious results. An external pressure probe would not be convenient neither due to its size and intrusion within the boundary layer. Nevertheless, some static pressure profiles measured in the near wake illustrate the strong impact of the blowing on the dynamics and are presented in part II.

3.2. Thermal profiles

The thermal behavior is found very similar to the dynamical one. The temperature profiles for a Reynolds number of 6000 are plotted in Figs. 8 and 9 for angles of 90° and 110° at 200°C and 100°C main flow temperatures, respectively. It can be observed that, with blowing, the thermal boundary layer thickens at all angles. When the angle is higher than the separation angle, an important quantity of cold fluid is present in the vicinity of

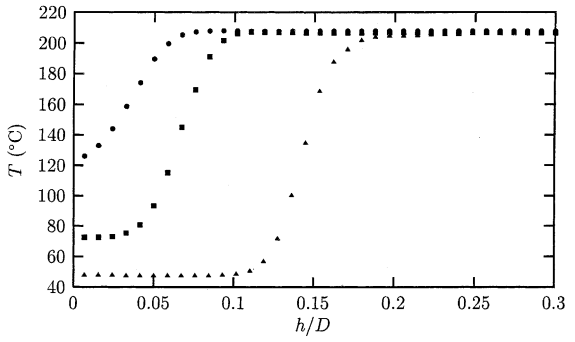

Fig. 8. Temperature profile at the top of the cylinder. $Re = 6000$, $\theta = 90°$, $T_\infty = 200°C$. ●, $F = 1\%$; ■, $F = 3\%$; ▲, $F = 10\%$.

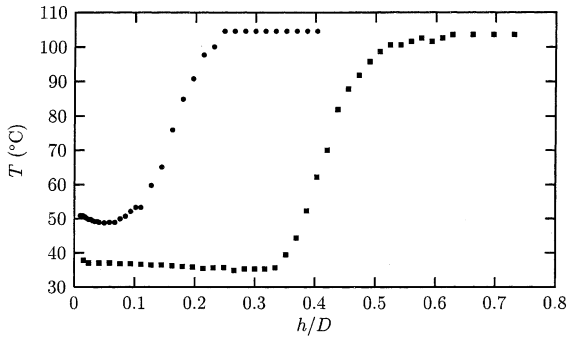

Fig. 9. Temperature profile along the vertical direction. $Re = 6000$, $\theta = 110°$, $T_\infty = 100°C$. ●, $F = 1\%$; ■, $F = 5\%$.

Table 2
Thermal boundary layer thickness evolution with blowing ($Re = 6000$, $\theta = 70°$)

F (%)	0.0	1.3	3.3	9.7
Δ/D	0.00	0.04	0.05	0.08

the cylinder wall, thus allowing an efficient thermal protection. For example, at $\theta = 90°$ with a 3% injection rate, the temperature remains below 75°C up to a position of $h/D = 0.03$, which corresponds to an important decrease and an effective protection of the surface in terms of convective heat flux.

We investigated the influence of the Reynolds number on the thermal profiles and the boundary layer. Same conclusions can be drawn as for the dynamical study where the Reynolds number is not an acting parameter (at least in the studied range).

Table 2 shows the thermal boundary layer thickness Δ for different injection rates at $\theta = 70°$ for a Reynolds number of 6000. Between 0% and 1.5%, it varies from 0 to 0.04 D, while it increases to 0.05 D for 3% and 0.08 D for 10%. When blowing occurs, a thermal boundary layer is developed, due to the mixing of two flows at different temperature (main and injected flow). Moreover, the wall temperature decreases, cooled by internal as well as external convections with the coolant.

4. Influence of the blowing on surface temperatures

In order to quantify the thermal impact of the blowing on the porous wall, we measured the surface temperature for different injection rates. In Fig. 10, the evolution of the wall temperature as a function of the angle for different injection rates and a main flow temperature of 250°C is shown. The highest temperature point is the front stagnation point ($\theta = 0°$) and the coldest is the rear stagnation point ($\theta = 180°$). For 1% of injection, a 30 K temperature difference between those points can be noted. Considering the hottest location, we can observe a 70 K decrease for 1% of injection compared to the no-blowing case. It should be noted that these temperature values are smoothed along the periphery by the internal heat conduction in the cylinder, which tends to flatten the evolution of the surface temperature with the angle. Fig. 11 exhibits the wall temperature as a function of the injection rate at an angle of 80° and different Reynolds numbers. The temperature decreases with the injection rate and a reduction of 160 K is observed for an injection rate of 5%. The decrease of the temperature is very sharp for weak injection rates and tends to an asymptotic limit corresponding to the temperature of the injected fluid. A Reynolds number effect can be noted, which is again due to the internal heat conduction effect. For a same injection rate but a higher Reynolds number, the coolant mass flow rate increases while the convective heat transfer coefficient remains low beyond the separation angle. The increasing coolant flow rate is not compensated by a thinner thermal boundary layer as it is the case in the upstream part of the cylinder. It results in a

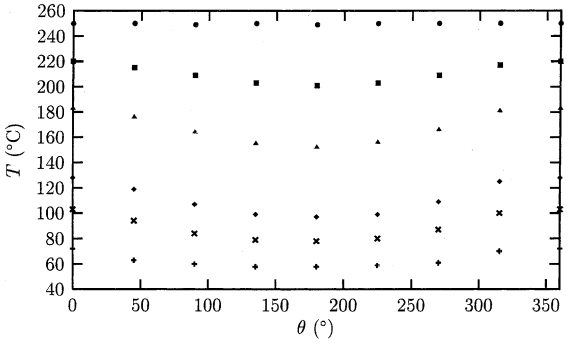

Fig. 10. Wall temperature distribution around the cylinder. $Re = 3900$, $T_\infty = 250°C$. ●, $F = 0\%$; ■, $F = 0.5\%$; ▲, $F = 1\%$; ◆, $F = 2\%$; ×, $F = 3\%$; +, $F = 4.5\%$.

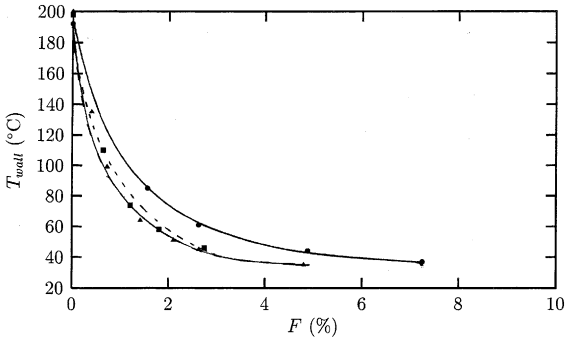

Fig. 11. Wall temperature evolution with blowing. $\theta = 80°$, $T_\infty = 200°C$. •, $Re = 3900$; ▪, $Re = 7000$; ▲, $Re = 10\,500$.

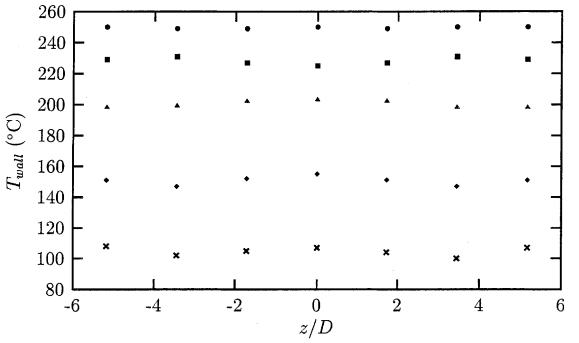

Fig. 13. Wall temperature distribution along the spanwise direction. $Re = 3900$, $\theta = 90°$, $T_\infty = 250°C$. •, $F = 0\%$; ▪, $F = 0.2\%$; ▲, $F = 0.5\%$; ◆, $F = 1\%$; ×, $F = 1.7\%$.

lower rear temperature, which tends, through internal heat conduction, to lower the upstream surface temperature as well.

In non-dimensional variable, the wall temperature is expressed as the thermal effectiveness, η, of the blowing defined as

$$\eta = \frac{T_\infty - T}{T_\infty - T_{\text{inj}}},$$

where T_∞, T and T_{inj} are the upstream, local and injected fluid temperature, respectively. The effectiveness is plotted in Fig. 12 for different main flow temperatures at $Re = 3900$ where it can be first observed that the thermal effectiveness increases with the injection rate and that the main flow temperature does not influence the effectiveness as the curves perfectly collapse. For a 2% injection, the effectiveness is close to 75% and rises almost up to 95% for a 5% blowing. The blowing efficiency is good as soon as the injection rate reaches a few percents and this illustrates one of the major advantages of the blowing technique. The efficiency limit reported here for 10% of injection is not 100% due to radiative heat transfer. Convective heat flux can be considered to be negligible for $F > 5\%$ while radiative heat transfer increases as the cylinder surface temperature decreases. Radiations thus become the predominant heat transfer mode for $F > 5\%$ while the cylinder is solely cooled by internal convection within the porous matrix.

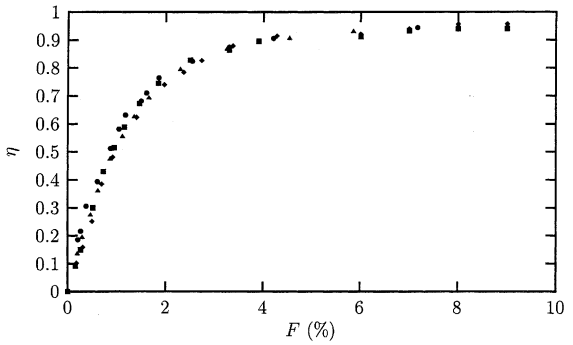

Fig. 12. Thermal protection effectiveness as a function of the blowing rate. $Re = 3900$. •, $T_\infty = 100°C$; ▪, $T_\infty = 150°C$; ▲, $T_\infty = 200°C$; ◆, $T_\infty = 250°C$.

Furthermore, the homogeneity of the cooling on the surface of the porous cylinder along the spanwise direction has been investigated. The temperature along the cylinder is measured at an angle of 90° for $T_\infty = 250°C$, at $Re = 3900$ and a blowing rate varying from 0% to almost 2%. Fig. 13 shows that the wall temperature remains the same and that three-dimensional wake patterns do not affect the spanwise temperature field. In particular, for this range of Reynolds number, the so-called three-dimensional near wake instability mode B occurs [19–21] and one could have questioned whether it can influence the upstream flow and the temperature field. Similar results have been obtained for other main flow temperatures and other Reynolds numbers.

5. Conclusions

The influence of the blowing through a porous circular cylinder in cross-flow on the main flow kinematics in the vicinity of the surface has been experimentally investigated. The blowing has been proved to strongly affect the boundary layers in terms of thickness and stability and to considerably promote their separation. The injection of low velocity fluid into the growing boundary layer increases its thickness, while lowering the normal gradients in the immediate vicinity of the surface. This results in a lower friction stress and a decrease in the viscous drag of the cylinder.

Thermal control applications have been studied with a hot main flow and a cold injected fluid (coolant). The thermal behavior of the flow is similar to the dynamical one and same conclusions can be drawn. The heat flux is found to be drastically reduced with blowing, as well as

the wall temperature. This thermal protection is effective for weak injection rates (roughly below 5%), even near the front stagnation point where the thermal stress is the highest due to a squashed boundary layer, thus leading to a strong heat transfer coefficient.

References

[1] S.V. Ekkad, J.C. Han, H. Du, Detailled film cooling measurements on a cylindrical leading edge model: effect of free-stream turbulence and coolant density, J. Turbomach. 120 (1998) 799–807.

[2] S.W. Lee, Y.B. Kim, J.S. Lee, Flow characteristics and aerodynamics losses of film-cooling jets with compounds angle orientations, J. Turbomach. 119 (1997) 310–319.

[3] R.J. Goldstein, L.D. Stone, Row-of-holes film cooling of curved walla at low injection angles, J. Turbomach. 119 (1997) 574–579.

[4] K. Funazaki, M. Yokota, S. Yamawaki, Effects of periodic wake passing on film effectiveness of discrete cooling holes around the leading edge of a blunt body, J. Turbomach. 119 (1997) 292–301.

[5] E.R.G. Eckert, J.N.B. Livingood, Method for calculation of laminar heat transfer in air flow around cylinders of arbitrary cross-section (including large temperature differences and transpiration cooling), NACA Report 1118, 1953, pp. 223–251.

[6] B.V. Johnson, J.P. Hartnett, Heat transfer from a cylinder in crossflow with transpiration cooling, J. Heat Transfer (1963) 173–179.

[7] E.R.G. Eckert, J.N.B. Livingood, Comparison of effectiveness of convection-, transpiration-, and film-cooling methods with air as coolant, NACA TN 3010, Report 1182, 1954, pp. 593–609.

[8] T.A. Ghee, J.G. Leishman, Unsteady circulation control aerodynamics of a circular cylinder with periodic jet blowing, AIAA J. 30 (2) (1992) 289–299.

[9] O. Cadot, M. Lebey, Shear instability inhibition in a cylinder wake by local injection of a viscoelastic fluid, Phys. Fluids 11 (2) (1999) 494–496.

[10] T. Hayashi, F. Yoshino, R. Waka, The aerodynamic characteristics of a circular cylinder with tangential blowing in uniform shear flows, JSME Int. J. series B 36 (1) (1993) 101–112.

[11] M. Amitay, J. Cohen, Instability of a two-dimensional plane wall jet subjected to blowing or suction, J. Fluid Mech. 344 (1997) 67–94.

[12] J.-C. Lin, J. Towfighi, D. Rockwell, Near-wake of a circular cylinder: control by steady and unsteady surface injection, J. Fluids Struct. 9 (1995) 659–669.

[13] J.C. Rodet, G.A. Campolina-Franca, P. Pagnier, R. Morel, A. Lallemand, Etude en soufflerie thermique du refroidissement de parois poreuses par effusion de gaz, Rev. Gén. Therm. 37 (1997) 123–136.

[14] H.H. Bruun, in: Hot-wire Anemometry. Principles and Signal Analysis, Oxford University Press, Oxford, 1995, p. 507.

[15] F. Bataille, J.C. Rodet, A. Lallemand, Experimental measurements of turbulent properties in a boundary layer with blowing, Turbulent Shear Flow Phenomena, Santa Barbara, 1999.

[16] J. Bellettre, F. Bataille, J.C. Rodet, A. Lallemand, Thermal behavior of porous plates subjected to air blowing, AIAA J. 14 (4) (2000) 523–532.

[17] J. Bellettre, F. Bataille, A. Lallemand, A new approach for the study of the turbulent boundary layer with blowing, Int. J. Heat Mass Transfer 42 (1999) 2905–2920.

[18] M.M. Zdravkovich, in: Flow Around Circular Cylinders Fundamentals, Oxford University Press, Oxford, 1997, p. 672.

[19] C.H.K. Williamson, The existence of two stages in the transition to three-dimensionaly of a cylinder wake, Phys. Fluids 31 (11) (1988) 3165–3168.

[20] M. Brede, H. Eckelmann, D. Rockwell, On secondary vortices in the cylinder wake, Phys. Fluids 8 (8) (1996) 2117–2124.

[21] C.H.K. Williamson, Three-dimensional wake transition, J. Fluid Mech. 328 (1996) 345–407.